Mol. Cryst. Liq. Cryst., Vol. 521: pp. 293–300, 2010

ISSN: 1542-1406 print/1563-5287 online
DOI: 10.1080/15421401003716155

Taylor & Francis
Taylor & Francis Group

Magnetic Properties of Cobalt Nanowire Arrays

ROBERTO LAVÍN,[1,2] JULIANO C. DENARDIN,[1,3] ANDREA CORTÉS,[4] HUMBERTO GÓMEZ,[5] MANUEL CORNEJO,[6] AND GUILLERMO GONZÁLEZ[6]

[1]Departamento de Física, Universidad de Santiago de Chile, USACH, Santiago, Chile
[2]Facultad de Ingeniería, Universidad Diego Portales, UDP, Santiago, Chile
[3]Centro para el Desarrollo de la Nanociencia y Nanotecnología, CEDENNA, Santiago, Chile
[4]Departamento de Física, Universidad Técnica Federico Santa María, Valparaíso, Chile
[5]Instituto de Química, Universidad Católica de Valparaíso, Valparaíso, Chile
[6]Departamento de Química, Universidad de Chile, Santiago, Chile

Arrays of Co nanowires with different lengths and diameters have been prepared by electrodeposition into nanopores of alumina and polycarbonate membranes. The dependence of the coercivity and remanence of the arrays as a function of the length, the electrodeposition potential, and the electrolytic bath pH of the nanowires has been experimentally investigated through hysteresis curves performed in a VSM (vibrating sample magnetometer) and a SQUID (superconducting quantum interference device).

Keywords Cobalt nanowires; electrodeposition; magnetic properties

Introduction

The study of arrays of magnetic nanowires is a topic that has attracted considerable interest due to their promising technological applications [1–4] mainly in high-density information storage. Electrodeposition in polycarbonate and alumina membranes is the preferred technique used in the fabrication of these systems [5,6]. In particular, highly ordered arrays of magnetic nanowires produced inside the pores of anodic alumina membranes by electrochemical deposition [6] have been the focus of intense research [7–10]. Different groups have investigated the stable magnetic configurations in function on the aspect ratio of the magnetic cylinders

Address correspondence to Roberto Lavín, Facultad de Ingeniería, Universidad Diego Portales, Ejército 441, Santiago, Chile. Tel.: 56-2-6762418; Fax: 56-2-6762402; E-mail: roberto.lavin@udp.cl

[11,12], the reversion mechanisms of the magnetization in nanowires [13,14], the influence of magnetostatic interactions among nanowires [15–17], and in general, the behavior of the magnetic properties in function of different parameters [18–20]. This paper shows the influence of the electrodeposition potential, electrolytic bath pH, length and diameter of Co nanowire arrays electrodeposited in alumina and polycarbonate membranes.

Experimental Method

The anodic aluminum oxide (AAO) membranes were prepared from a 99.99% aluminum foil (0.13 mm thickness, SIGMA-ALDRICH) by the two-step anodization technique as described in the reference [21]. The grease on the aluminum surface was removed with detergent, then successively with acetone and water. The cleaned aluminum sheets were submitted to an annealing at 350°C in air during 1 hour, using a Lindgerg/Blue M model tube furnace. Next, the aluminum sheets were first etched with a 5% w/w NaOH solution and afterwards with diluted nitric acid. Subsequently, the samples were mechanically polished with alumina (0.30 and 0.05 μm mesh) followed by 1 minute of electropolishing at 15 V in a 40% H_2SO_4, 59% H_3PO_4, 1% glycerine bath. After this treatment, the samples were submitted to a first anodization at 40 V during 6 hours in a 0.3 M oxalic acid solution at 20°C. The anodized layer was etched with a 5% H_3PO_4, 1.8% $H_2Cr_2O_4$ solution at room temperature during 12 hours. The ordered pore arrangement was achieved with a second anodization step that was performed under the same conditions as in the first one. A 0.10 M $CuCl_2$, 20% v/v HCl solution at room temperature was employed to remove the remaining aluminum from the alumina substrate. To remove the barrier layer and to open the pores at the bottom, the membrane was first treated with 5% H_3PO_4 and 5% NaOH aqueous solution at room temperature. Subsequently, the pores were widened in a 0.085 M H_3PO_4 solution at 37°C for 15 min. To facilitate the electric contact, a very thin Au-Pd layer was sputtered on one side of the membrane followed by the electrodeposition of a thicker copper layer for achieving the full pore sealing.

The electrochemical depositions were performed with an IM6e BAS-ZAHNER potentiostat controlled through a PC. The electrochemical cell consisted in a three electrode arrangement with the AAO as working electrode, a platinum foil as counter-electrode, and Ag/AgCl(sat) as reference. The cobalt nanowires were deposited under potentiostatic control at room temperature in an unstirred electrolyte solution containing 0.4 M $CoSO_4 + 0.28$ M H_3BO_3 at $pH = 2$ and $pH = 4$.

The magnetization measurements were performed by a vibrating sample magnetometer (VSM) and a superconducting quantum interference device (SQUID). We have realized our measurements at ambient temperature.

Results and Discussion

Nanowires in Alumina Template

The morphological characterization of the AAO was made with a scanning electron microscope. As is observed in Figure 1, the membranes present highly ordered pores of diameter $d = 2r = 50$ nm and lattice constant $D = 100$ nm.

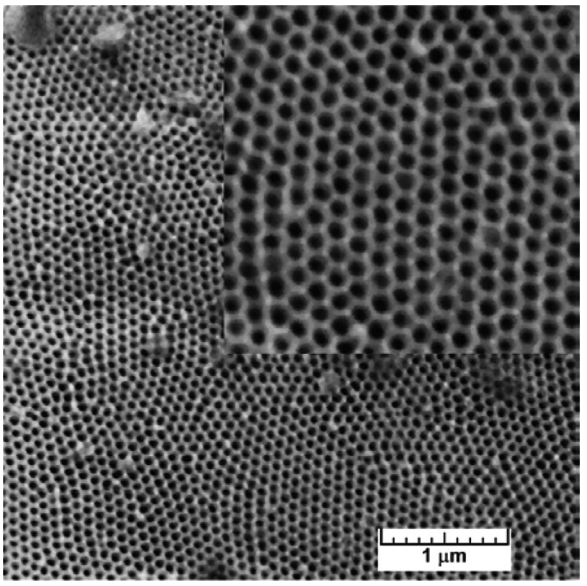

Figure 1. SEM top view of a highly ordered home-made AAO template. The inset shows the magnification of the image.

Figure 2 shows the hysteresis loops with the external field H, parallel ($H\|$) and perpendicular ($H\perp$) to the nanowires axis, for samples with lengths of $L = 4$ and $10\,\mu m$, at ambient temperature. The difference between the parallel and perpendicular hysteresis loops defines the uniaxial anisotropy; the coercivity and remanence in the parallel configuration are larger than in the perpendicular configuration, indicating that the magnetic easy axis is along the nanowire axis. The magnetic behavior of magnetic nanowire arrays is strongly dependent on the magnetic anisotropies

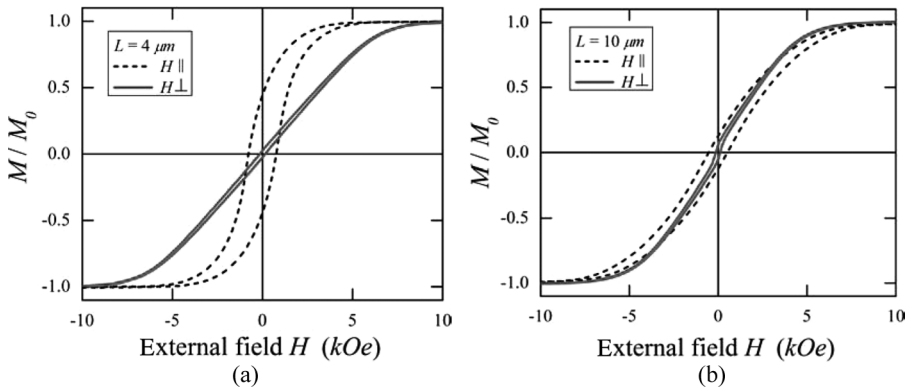

Figure 2. Normalized hysteresis curves with the external magnetic field parallel ($H\|$) and perpendicular ($H\perp$) to the nanowire axis, for two different lengths of nanowires: (a) $L = 4\,\mu m$ and (b) $L = 10\,\mu m$. Both samples have the same parameters: electrodeposition potential, electrolytic bath pH, diameter, and interpore distance.

(mainly the shape and crystalline anisotropy) and the dipolar interaction between nanowires [19]. In nanowires with a large aspect ratio (L/d) the shape anisotropy will induce a magnetic easy axis parallel to the nanowire axis, and it is expected that the easy axis will lie along the nanowire axis, as can be observed in Figure 2(a). In contrast, the dipolar interaction (that is dependent on the length of the nanowires) will induce a magnetic easy axis perpendicular to the nanowire axis [19]. This causes that for arrays with very long nanowires, the dipolar interaction will overcome the effect of the shape anisotropy and will decrease the coercivity and remanence, as can be observed in Figure 2(b).

For the array of length $L = 4\,\mu m$ the coercivity measured with the external field along and perpendicular to the axis of the nanowires changes from to $H_c^{\parallel} = 750$ Oe to $H_c^{\perp} = 150$ Oe respectively, while for $L = 10\,\mu m$ changes from to $H_c^{\parallel} = 550$ Oe to $H_c^{\perp} = 120$ Oe. Thus, the magnetic properties presented in this work (especially for the array with length $L = 4\,\mu m$) are very suitable for applications in information storage media [7, 22].

We have also investigated the effect of the electrodeposition potential, V, and the electrolytic bath pH on the magnetic properties of the samples. Figure 3 shows the influence of the electrodeposition potential for electrolytic bath pH of 2.0 and 4.0. It is observed that the different electrodeposition potentials lead to different aspect ratios of the hysteresis curves. It has been observed that changes in the electrodeposition potential results in the formation of nanowires with different crystallographic structures [23]. One can also observe that the influence of the electrodeposition potential is smaller for nanowires that are longer (Fig. 3(b)).

The effective magnetic anisotropy of the nanowire arrays is determined by four contributions: (i) the shape anisotropy, which will induce a magnetic easy axis parallel to the nanowire axis, (ii) the dipolar interaction between nanowires, which will induce a magnetic easy axis perpendicular to the nanowire axis, (iii) the crystalline anisotropy and (iv) the magnetoelastic anisotropy, due to stress between the template and the nanowires, which will induce a magnetic easy parallel or perpendicular to the

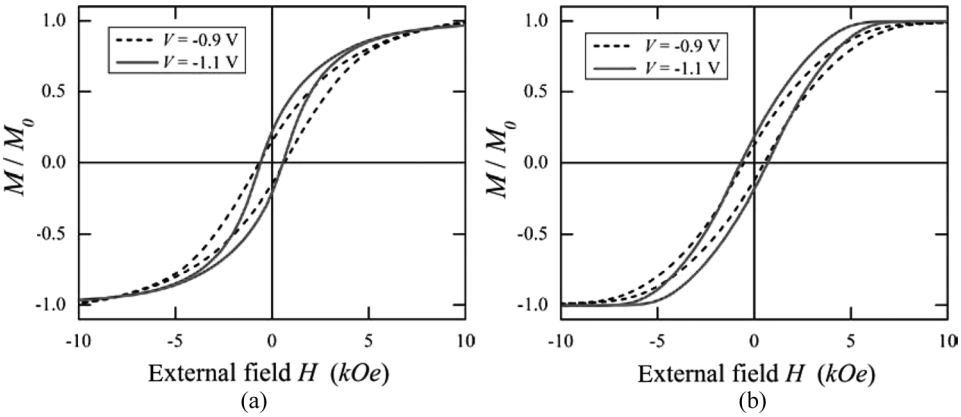

Figure 3. Normalized hysteresis curves as function of the electrodeposition potential, for (a) $L = 4\,\mu m$ and pH = 4, and (b) $L = 9\,\mu m$ and pH = 2. Both samples have the same nanowire diameter $d = 50$ nm and interpore distance $D = 100$ nm. The external magnetic field is applied parallel to the nanowire axis.

stress direction. In Co nanowires the contribution of the magnetoelastic anisotropy at ambient temperature is negligible compared to other anisotropies terms [24,25]. Thus, the effective anisotropic field of a Co nanowire array is

$$H_k = 2pM_0 - 6.3\pi M_0 r^2 L/D^3 + H_{cris}, \tag{1}$$

were M_0 is the saturation field, r is the radius of nanowires, D is the separation between nanowires, and L is the nanowire length [19]. The first term in Eq. (1) is the shape anisotropy field, the second term is the dipolar field acting on one nanowire due to all other nanowires in the array, and the third term is the crystalline anisotropy field, that is dependent on the growth conditions of the nanowires (electrodeposition conditions) [23]. This expression predicts that the H_k decreases as the nanowires length increases, as our experimental results demonstrate (see Fig. 2). Figure 4 shows the coercivity and the remanence as function of the length of the nanowires, and for different synthesis conditions. In general there is a decrease of the coercivity and remanence with the increase of the length of the nanowires, for all growing conditions. This behavior is in good agreement with the prediction of Eq. (1) and is opposed to the effect observed in Ni nanowire arrays [15].

Nanowires in Polycarbonate Membranes

In order to investigate the magnetic properties of nanowires with larger diameters we have electrodeposited Co nanowires on commercial polycarbonate membranes, with average pore diameters of 200 nm. Figure 5 shows SEM images of the nanowires with average diameter of 200 nm and lengths of 6 μm.

In Figure 6 it is shown the hysteresis curves for Co nanowire arrays with diameter $d \approx 200$ nm and $L \approx 6$ μm electrodeposited in a polycarbonate membrane. The coercivities in the two configurations (parallel and perpendicular) are similar,

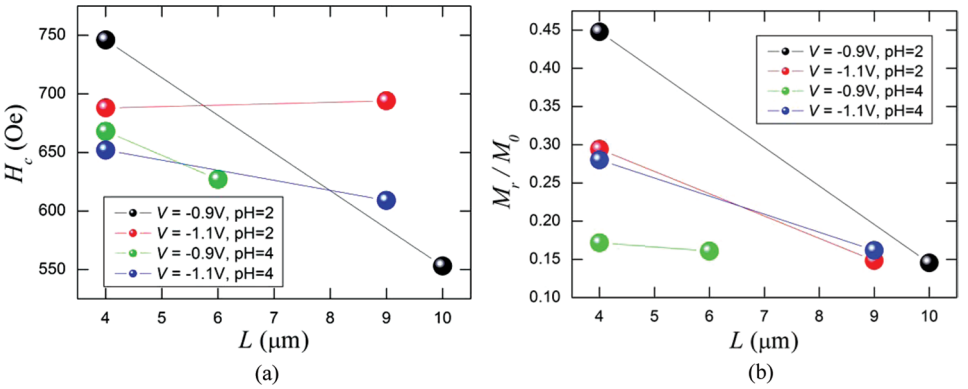

Figure 4. (a) Coercivity (H_c) and (b) squareness (M_r/M_0) of nanowires arrays growth at different electrochemical conditions and as a function of length: (i) $V = -0.9$ V, pH = 2.0, (ii) $V = -0.9$ V, pH = 4.0, (iii) $V = -1.1$ V, pH = 2.0, and (iv) $V = -1.1$ V, pH = 4.0. All samples have the same nanowires diameter $d = 50$ nm and interpore distance $D = 100$ nm. The external magnetic field is applied parallel to the nanowire axis.

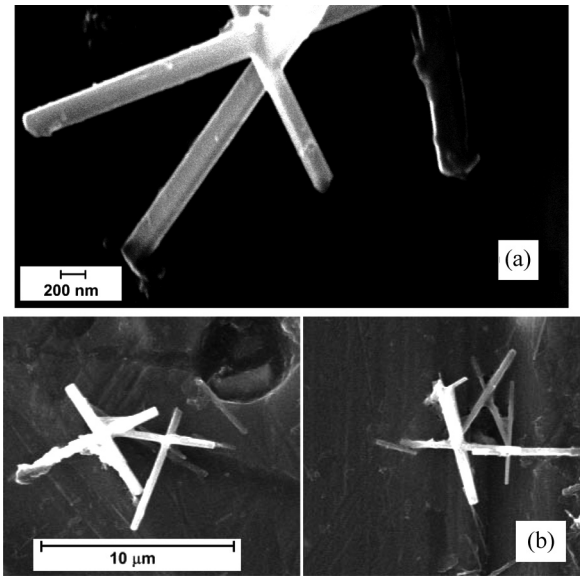

Figure 5. SEM image of free standing nanowires synthesized trough electrodeposition in polycarbonate membranes: (a) magnification: 60000× and (b) magnification 5000×.

with $H_c^{\|} = 125$ Oe and $H_c^{\perp} = 100$ Oe. However, the squareness in the perpendicular configuration is larger than in the parallel configuration, $(M_r/M_0)_{\|} = 0.11$ and $(M_r/M_0)_{\perp} = 0.26$. This is opposite to the effect observed in nanowire arrays electrodeposited in alumina membranes with diameter $d = 50$ nm (see Fig. 2). Therefore, in nanowires with $d \approx 200$ nm, the magnetic easy axis becomes perpendicular to the nanowire axis. This variation in the alignment of easy axis in nanowires with 200 nm in diameter can be attributed to the dependence of the magnetic anisotropy

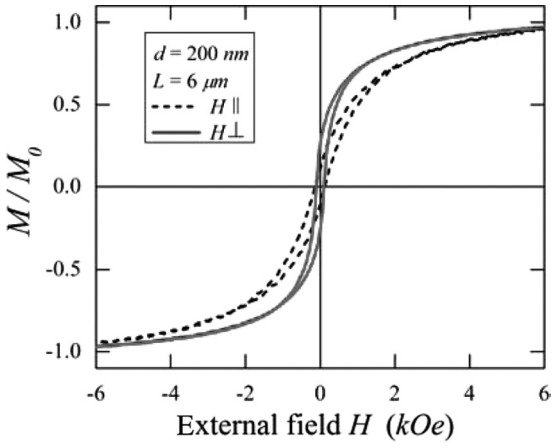

Figure 6. Normalized hysteresis curves with the external magnetic field parallel ($H\|$) and perpendicular ($H\perp$) to the nanowire axis, for Co nanowires electrodeposited in a polycarbonate membrane, with diameter $d \approx 200$ nm, and $L \approx 6\,\mu$m (see Fig. 5).

as a function of the diameter of the nanowires and also in the dependence of the magnetic interactions as function of the radius of the nanowires (Eq. (1)).

Conclusion

Highly ordered Cobalt nanowire arrays with different lengths and diameters of nanowires, were successfully fabricated by electrochemical deposition in alumina template with pore diameter $d = 50$ nm and interpore distance $D = 100$ nm, and in polycarbonate membranes with pore diameters of $d = 200$ nm. The electrodeposition potential V and pH also were varied in order to observed the influence of these parameters on the magnetic properties of the arrays. The increases of length the nanowires result in the decrease of the coercivity and remanence in nanowires of diameter $d = 50$ nm, for almost all combinations of the electrodeposition potential and pH. In cobalt nanowires with a mean diameter of $d = 200$ nm, fabricated by electrochemical deposition in polycarbonate membranes, the easy axis becomes perpendicular to the nanowires axis.

In conclusion, in Co nanowire samples the magnetic anisotropy is dependent of the electrodeposition potential, the electrolytic bath pH, nanowire length and diameter. Therefore, the magnetic properties of interest (coercivity and remanence) can be adjusted by controlling these parameters.

Acknowledgments

This work was supported by the Proyecto Fondecyt Postdoctorado (Grant No. 3100117), the Financiamiento Basal para Centros Científicos y Tecnológicos de Excelencia (CEDENNA), the Millennium Science Nucleus *Basic and Applied Magnetism* (Grant No. P06-022F), and the Fondecyt (Grants No. 1080164 and 3080058).

References

[1] Koch, R. H., Deak, J. G., Abraham, D. W., Trouilloud, P. L., Altman, R. A., Lu, Y., Gallagher, W. J., Scheuerlein, R. E., Roche, K. P., & Parkin, S. S. P. (1998). *Phys. Rev. Lett.*, *81*, 4512–4515.

[2] Cowburn, R. P., Koltsov, D. K., Adeyeye, A. O., Welland, M. E., & Tricker, D. M. (1999). *Phys. Rev. Lett.*, *83*, 1042–1045.

[3] Wolf, S. A., Awschalom, D. D., Buhrman, R. A., Daughton, J. M., von Molnar, S., Roukes, M. L., Chtchelkanova, A. Y., & Treger, M. (2001). *Science*, *294*, 1488–1495.

[4] Gerrits, Th., van der Berg, H. A. M., Hohlfeld, J., Bar, L., & Rasing, Th. (2002). *Nature*, *418*, 509–512.

[5] Motoyama, M., Fukunaka, Y., Sakka, T., & Ogata, Y. H. (2008). *Electrochimica Acta*, *53*, 5766–5773.

[6] Masuda, H. & Fukuda, K. (1995). *Science*, *268*, 1466.

[7] Nielsch, K., Wehrspohn, R. B., Barthel, J., Kirschner, J., Gösele, U., Fischer, S. F., & Kronmülle, H. (2001). *Appl. Phys. Lett.*, *79*, 1360.

[8] Wang, Z. K., Lim, H. S., Zhang, V. L., Goh, J. L., Ng, S. C., Kuok, M. H., Su, H. L., & Tang, S. L. (2006). *Nano Lett.*, *6*, 1083–1086.

[9] Escrig, J., Altbir, D., Jaafar, M., Navas, D., Asenjo, A., & Vázquez, M. (2007). *Phys. Rev. B*, *75*, 184429.

[10] Liu, M., Lagdani, J., Imrane, H., Pettiford, C., Lou, J., Yoon, S., Harris, V. G., Vittoria, C., & Sun, N. X. (2007). *Appl. Phys. Lett.*, *90*, 103105.

[11] Ross, C. A., Hwang, M., Shina, M., Cheng, J. Y., Farhoud, M., Savas, T. A., Smith, H. I., Schwarzacher, W., Ross, F. M., Redjal, M., & Humphrey, F. B. (2002). *Phys. Rev. B*, *65*, 144417.
[12] Landeros, P., Escrig, J., Altbir, D., Laroze, D., d'Alburquerque e Castro, J., & Vargas, P. (2005). *Phys. Rev. B*, *71*, 094435.
[13] Kröll, M., Blau, W. J., Grandjean, D., Benfield, R. E., Luis, F., Paulus, P. M., & de Jongh, L. J. (2002). *J. Magn. Magn. Mater.*, *249*, 241–245.
[14] Foster, H., Schrefl, T., Suess, D., Scholz, W., Tsiantos, V., Dittrich, R., & Fidler, J. (2002). *J. Appl. Phys.*, *91*, 6914.
[15] Escrig, J., Lavín, R., Palma, J. L., Denardin, J. C., Altbir, D., Cortés, A., & Gómez, H. (2008). *Nanotechnology*, *19*, 075713.
[16] Lavín, R., Denardin, J. C., Escrig, J., Altbir, D., Cortés, A., & Gómez, H. (2008). *IEEE Trans. Magn.*, *44*, 2808.
[17] Hertel, R. (2001). *J. Appl. Phys.*, *90*, 5752.
[18] Inguanta, R., Piazza, S., & Sunseri, C. (2006). *Electrochim. Acta*, *53*, 5766–5773.
[19] Han, G. C., Zong, B. Y., Luo, P., & Wu, Y. H. (2003). *J. Appl. Phys.*, *93*, 9202.
[20] Duan, J., Liu, J., Cornelius, T. W., Yao, H., Mo, D., Chen, Y., Zhang, L., Sun, Y., Hou, M., Trautmann, C., & Neumann, R. (2009). *Nucl. Instru. Meth. Phys. B*, *267*, 2567–2570.
[21] da F. Costa, L., Riveros, G., Gómez, H., Cortés, A., Pilles, M., Dalchiele, E. A., & Marotti, R. E. (2005). http://arxiv.org/abs/cond-mat/0504573.
[22] Nielsch, K., Wehrspohn, R. B., Barthel, J., Kirschner, J., Fischer, S. F., Kronmüller, H., Schweinböck, T., Weiss, D., & Gösele, U. (2002). *J. Magn. Magn. Mater.*, *249*, 234–240.
[23] Cortés, A., Lavín, R., Denardin, J. C., Gómez, H., Marotti, R. E., & Dalchiele, E. A. (2009). Template assisted electrochemical growth cobalt nanowires: Study of the influenced of the deposition conditions on structural and optical properties. Submitted.
[24] Pirota, K. R., Silva, E. L., Zanchet, D., Navas, D., Vázquez, M., Hernández-Vélez, M., & Knobel, M. (2007). *Phys. Rev. B*, *76*, 233410.
[25] Silva, E. L., Nunes, W. C., Knobel, M., Denardin, J. C., Zanchet, D., Pirota, K., Navas, D., & Vázquez, M. (2006). *Physica B*, *384*, 22–24.